Band Structure of Beryllium by the Augmented-Plane-Wave Method*

J. H. TERRELL†‡
Department of Physics, Brandeis University, Waltham, Massachusetts
and
Solid-State and Molecular Theory Group, Massachusetts Institute of Technology, Cambridge, Massachusetts
(Received 9 August 1965; revised manuscript received 25 March 1966)

The results of an augmented-plane-wave (APW) calculation of hexagonal-close-packed beryllium are presented in the form of the Fermi energy, energy bands which were extended to energies much higher than the Fermi energy, density-of-states curve below the Fermi energy, and electronic specific heat. The crystalline potential used in calculating the energy bands was obtained by superposing self-consistent Hartree-Fock atomic-beryllium potentials on first-, second-, and third-nearest neighbors, and exchange was treated in the Slater free-electron-exchange approximation. The good agreement between the theoretically and experimentally determined Fermi surfaces which was found previously by the author is discussed. The general features of the density-of-states curve for energies below the Fermi energy are in good agreement with the soft-x-ray emission data, and the electronic specific heat coefficient is in reasonable agreement with published experimental results. The energy bands of hcp beryllium and hcp magnesium are discussed by comparing the logarithmic derivatives of their respective wave functions across the respective APW sphere radii. The results of comparing the logarithmic derivatives of beryllium and magnesium are used to emphasize the close connection between orthogonalized-plane-wave and APW methods.

1. INTRODUCTION

THE results of an augmented-plane-wave (APW) calculation on hexagonal-close-packed (hcp) beryllium are presented. Energy eigenvalues which converged to 0.001 Ry were computed at 45 points in 1/24 of the Brillouin zone (B.Z.). The Fermi energy was determined by using graphically interpolated energy eigenvalues which were found at the equivalent of 1152 points in the B.Z. with an estimated error of less than 0.01 Ry. The Fermi surface was constructed from the intersections of these energy bands with the Fermi energy and comparison with the experimentally determined Fermi surface according to Watts[1] has been made previously by the author.[2] The agreement between the Fermi surface constructed from these energy bands and the experimentally determined Fermi surface was found to be quite good, and we discuss the differences which were found. A density-of-states curve was constructed for energies below the Fermi energy, the general features of which are in good agreement with the soft-x-ray emission data of Johnston and Tomboulian.[3] The electronic specific heat was found to be in reasonable agreement with the experimental results of Hill and Smith[4] and Gmelin.[5] Although the energy eigenvalues and energy bands have been extended a good deal above the Fermi energy, we have made no attempt to construct a density of states for energies greater than the Fermi energy. The energy bands of hcp beryllium that we find are compared to the energy bands of hcp magnesium according to Falicov[6] in the light of their respective Fermi surfaces and the matching of the logarithmic derivatives of their respective wave functions across the APW sphere radii. We use the results of comparing the logarithmic derivatives of beryllium and magnesium to emphasize the close connection between the orthogonalized-plane-wave (OPW) method and the APW method.

Herring and Hill[7] first discussed the band structure of beryllium by the OPW method. They computed energy eigenvalues at points of high symmetry in the B.Z. and found a density of states, Fermi energy, and a value for the electronic specific heat. It is useful to have an independent calculation of the same material by a different method; and since the APW method has been used successfully in determining energy bands, it was considered worthwhile to calculate the energy bands of beryllium by the APW method. Moreover, computer techniques developed by Saffren[8] and Wood[9] have greatly increased the ease of applying the APW method. While this calculation was being completed, Watts[1] proposed a Fermi surface for beryllium based on his de Haas–van Alphen experiments and pointed out that a Fermi surface based on Herring and Hill's calculation would be qualitatively similar to the experimentally determined Fermi surface if the Fermi energy is chosen to be slightly different from the one calculated by Herring and Hill. This result stimulated interest in arriving at a theoretically determined Fermi surface for which detailed comparison with the experimentally determined Fermi surface could be made. The theoretically determined Fermi surface was constructed by

* Work performed at MIT supported by the U. S. Office of Naval Research and the National Science Foundation.
† Supported by the National Science Foundation (NSF-F19994) and the U. S. Army Research Office, Durham (ARO-G233).
‡ Present address: Mithras, Inc., 701 Concord Avenue, Cambridge, Massachusetts 02138.
[1] B. R. Watts, Phys. Letters **3**, 284 (1963).
[2] J. H. Terrell, Phys. Letters **8**, 149 (1964).
[3] R. W. Johnston and D. H. Tomboulian, Phys. Rev. **94**, 1585 (1954). See also references to other x-ray data in the paper of Loucks and Cutler (Ref. 11).
[4] R. Hill and P. Smith, Phil. Mag. **44**, 636 (1953).
[5] M. E. Gmelin, Compt. Rend. **259**, 3459 (1964).
[6] L. M. Falicov, Phil. Trans. Roy. Soc. London **A255**, 55 (1962).
[7] C. Herring and A. G. Hill, Phys. Rev. **58**, 132 (1940).
[8] M. M. Saffren, Ph.D. thesis, MIT, 1959 (unpublished).
[9] J. H. Wood, Phys. Rev. **117**, 714 (1960).

the author[2] using the results of this calculation and is made up of a hole region and an electron region. The hole region is in the form of a closed six-cornered coronet connected by tiny necks. The electron region is in the form of two cigars each with a triangular midsection which becomes circular as one moves toward the ends. There is also a slight indentation at the midsection. Reference to the free-electron Fermi surface constructed by Harrison[10] reveals that significant distortions in the free-electron case have occurred for the Fermi surface of beryllium.

Loucks and Cutler[11] carried out another OPW calculation of beryllium finding the energy eigenvalues at the equivalent of 5184 points in the B.Z. From this they found the Fermi energy, the density of states, a value for the electronic specific heat, and the Fermi surface. The theoretically determined Fermi surface found by Loucks and Cutler is very similar to the one found by the author, and both compare favorably with the experimentally determined Fermi surface of Watts. Watts has recently compared the theoretically determined Fermi surfaces found by the author and by Loucks and Cutler with the Fermi surface found by the de Haas–van Alphen effect.[12] Other band calculations of beryllium have appeared,[13] but they do not allow accurate comparisons to be made with the latest experimental results.

The potential used in this calculation is described in Sec. 2 along with a brief discussion of the APW method. Exchange was included by the Slater free-electron-exchange approximation.[14] The results of this calculation are presented in Sec. 3 in the form of the energy bands, density-of-states curve, and electronic specific heat. The features of the Fermi surface found by the author[2] are discussed in Sec. 3 in terms of the energy bands and Fermi energy. Drawings of the Fermi surface along with detailed numerical comparisons with the experimental results of Watts[1] are given in Ref. (2) and are not reproduced here. The theoretically determined Fermi surface found by the author is discussed in relation to the theoretically determined Fermi surface found by Loucks and Cutler and the experimentally determined Fermi surface found by Watts. In Sec. 4 the energy bands of hcp beryllium are compared to the energy bands of hcp magnesium according to Falicov[6] in terms of their respective Fermi surfaces and in terms of the logarithmic derivatives of the respective wave functions at the APW sphere radii. A discussion of these results from the viewpoint of the OPW cancellation theorem of Cohen and Heine[15] is then given, and we emphasize the close connection of the APW method with the psuedopotential method of Heine and Abarenkov.[16]

2. APW METHOD AND POTENTIAL

In order to obtain convergence in the energy eigenvalue solutions to the Hartree-Fock equation, the choice of basis sets is important, i.e., the Bloch[17] wave function must be expanded in a set of functions which will lead to rapid convergence in energy. One possible choice of basis function is the OPW and another is the APW. The APW method was proposed by Slater[18] and extended by Saffren and Slater.[19] The APW method has become successful in recent years for determining band structures; and for a description of the APW method, its relation to other energy band methods, and the associated literature, the interested reader is referred to the recent book by Slater.[20]

The details of calculating the energy eigenvalues using the APW method will not be reproduced here. Wood[9] has given a detailed discussion of the method of computation which has been employed. The ijth matrix element for two atoms per unit cell and for the αth irreducible representation is as follows:

$$(H-E)_{ij}{}^{\alpha}=(g/h)\sum_{R}\Gamma_{\alpha}{}^{*}(R)_{ll'}\langle\phi_i|H-E|R\phi_j\rangle$$

$$=(g/h)\sum_{R}\Gamma_{\alpha}{}^{*}(R)_{ll'}\Big\{(\mathbf{k}_i\cdot R\mathbf{k}_j-E)\delta_{\mathbf{k}_i,R\mathbf{k}_j}+\frac{1}{\Omega}2\cos[(R\mathbf{k}_j-\mathbf{k}_i)\cdot\mathbf{r}_n]F_{ij}\Big\}.$$

$$F_{ij}=4\pi R_s{}^{2}\Big\{-(\mathbf{k}_i\cdot R\mathbf{k}_j-E)\frac{j_1(|R\mathbf{k}_j-\mathbf{k}_i|R_s)}{|R\mathbf{k}_j-\mathbf{k}_i|}+\sum_{l=0}^{\infty}(2l+1)P_l\Big(\frac{\mathbf{k}_i\cdot R\mathbf{k}_j}{|\mathbf{k}_i||\mathbf{k}_j|}\Big)\times j_l(k_iR_s)j_l(k_jR_s)\frac{u_l'(R_s,E)}{u_l(R_s,E)}\Big\}.$$

The hcp structure is a nonsymmorphic space group and the sum on the operators R include nonprimitive translations.

The origin is at the inversion center of the hcp lattice and $\mathbf{r}_n$ is the coordinate of one of the atoms in the unit cell. The symmetry of the hcp lattice with this choice of coordinate system has been discussed by Slater.[20] The order of the group of the wave vector is labeled g, and h is the dimension of the αth irreducible representation. The $u_l(R_s,E)$ are solutions to the radial Schrödinger equation within a sphere of radius R_s for energy E using the spherical potential described below. The other

[10] W. A. Harrison, Phys. Rev. **118**, 1190 (1960).
[11] T. L. Loucks and P. H. Cutler, Phys. Rev. **133**, A819 (1964).
[12] B. R. Watts, Proc. Roy. Soc. (London) **A282**, 521 (1964).
[13] J. F. Cornwell, Proc. Roy. Soc. (London) **A261**, 551 (1961); R. Jacques, Cahiers Phys. **70**, 1 (1956); **71–72**, 31 (1956).
[14] J. C. Slater, *Quantum Theory of Atomic Structure* (McGraw-Hill Book Company, Inc., New York, 1960).
[15] M. H. Cohen and V. Heine, Phys. Rev. **122**, 1821 (1961).
[16] V. Heine and I. Abarenkov, Phil. Mag. **9**, 451 (1964).
[17] F. Bloch, Z. Physik **52**, 555 (1928).
[18] J. C. Slater, Phys. Rev. **51**, 846 (1937).
[19] M. M. Saffren and J. C. Slater, Phys. Rev. **92**, 1126 (1953).
[20] J. C. Slater, *Quantum Theory of Molecules and Solids* (McGraw-Hill Book Company, Inc., New York, 1965), Vol. II.

TABLE I. Potential for hcp beryllium. The radial distance r is in atomic units, and the constant potential between the spheres of radius R_s is -1.6998 Ry.

r	$-2Z_p(r)=rV(r)_{\text{crystal}}$	$rV(r)_{\text{exchange}}$	r	$-2Z_p(r)=rV(r)_{\text{crystal}}$	$rV(r)_{\text{exchange}}$
0.010	7.9281	0.0945	0.300	5.7580	1.3436
0.020	7.8519	0.1839	0.340	5.5420	1.3785
0.030	7.7726	0.2687	0.380	5.3437	1.3956
0.040	7.6908	0.3408	0.420	5.1603	1.3983
0.050	7.6072	0.4248	0.500	4.8293	1.3712
0.060	7.5225	0.4965	0.580	4.5355	1.3161
0.070	7.4371	0.5642	0.660	4.2723	1.2487
0.080	7.3514	0.6281	0.740	4.0389	1.1826
0.090	7.2659	0.6884	0.820	3.8384	1.1305
0.100	7.1808	0.7452	0.900	3.6753	1.1020
0.120	7.0130	0.8490	0.980	3.5511	1.1021
0.140	6.8496	0.9406	1.140	3.4035	1.1177
0.160	6.6916	1.0211	1.300	3.3443	1.3095
0.180	6.5395	1.0914	1.460	3.3345	1.4576
0.200	6.3938	1.1152	1.620	3.3360	1.6051
0.220	6.2545	1.2049	1.780	3.4213	1.7485
0.240	6.1215	1.2496	1.940	3.5215	1.8890
0.260	5.9946	1.2872	2.100	3.6663	2.0294
0.280	5.8736	1.3183	2.260	3.8609	2.1723

quantities are defined in the paper by Wood.[9] Convergence to 0.001 Ry in energy for each irreducible representation was achieved by adjusting through trial and error the number of APW functions together with the maximum l value in the sum on l in the above equation. A maximum value of $l=12$ was found to be good enough. By convergence tests it was found that about 21 plane waves were needed to obtain convergence.

The APW method requires a one-electron potential spherically symmetric within spheres of radius R_s centered on the atomic sites and constant between the spheres. R_s was chosen so that the spheres surrounding neighboring atoms touch, and $R_s=2.159$ atomic units (a.u.) where 1 a.u.$=0.529\times10^{-8}$ cm. This potential should, of course, resemble the one-electron potential due to the actual charge distribution as closely as possible.

The crystalline potential was found by superposing atomic potentials placed on first-, second-, and third-nearest neighbors, and a spherical average taken. The procedure for this has been discussed by Mattheiss.[21] The number of neighbors used for constructing the potential is based on an ideal c/a ratio. $a=4.319$ a.u. and $c=6.771$ a.u.[22] Although the c/a ratio for beryllium is not ideal, this is not expected to greatly affect the potential. The free-atom potential for the beryllium atom in the $(1s)^2(2s)^2$ state was taken from a self-consistent Hartree-Fock calculation by Clementi, Roothaan, and Yoshimine.[23] Exchange was calculated in the Slater free-electron-exchange approximation[14] using the summed spherical potential. Thus, symbolically we have $V(r)_{\text{crystal}}=V(r)_{\text{Coulomb}}+V(r)_{\text{exchange}}$. $V(r)_{\text{Coulomb}}$ is the spherical average of the total Coulomb potential at a lattice site from first-, second-, and third-nearest-neighbor beryllium atoms, and $V(r)_{\text{exchange}}=-6[3\rho(r)/8\pi]^{1/3}$. $\rho(r)$ is the spherically averaged charge distribution at first-, second-, and third-nearest-neighbor sites due to the $(1s)^2(2s)^2$ states of the beryllium atom. The potential is given in Table I. For atoms the Slater free-electron-exchange approximation is poor far from the nucleus where the charge density is small. In the case of solids one expects the approximation to be less severe in the sense that electrons move more or less independently of each other and therefore see the same potential. We mention two of the many calculations concerning the validity of the free-electron-exchange approximation: The main contribution to the exchange energy of an electron gas in a periodic potential was found by Eyges[24] to come from the plane-wave component of the wave function; according to Reitz[25] the exchange energy of valence electrons in monatomic metals is not altered much because of spatial variations of the ground-state wave functions. Furthermore, Mattheiss[26] demonstrated that quite reasonable bands for the iron transition series could be obtained with the APW method using the Slater free-electron-exchange approximation and spherically averaging the summed potentials as described above. Robinson *et al.*[27] suggested that electron correlations could be taken into account by screening the exchange potential calculated in the free-electron approximation. This procedure was considered desirable since the free-electron approximation can overestimate exchange at the low-density tails of atomic functions.[28] Screening would decrease sharply the potential in this region. On the other hand,

[21] L. F. Mattheiss, Phys. Rev. **133**, A1399 (1964).
[22] Room-temperature lattice parameters are from W. B. Pearson, *A Handbook of Lattice Spacings and Structures of Metals and Alloys* (Pergamon Press, Inc., New York, 1958).
[23] E. Clementi, C. C. J. Roothaan, and M. Yoshimine, Phys. Rev. **127**, 1618 (1962).
[24] L. Eyges, Phys. Rev. **130**, 2218 (1963).
[25] J. Reitz, J. Chem. Phys. **22**, 595 (1954).
[26] L. F. Mattheiss, Phys. Rev. **134**, A970 (1964).
[27] J. E. Robinson, F. Bassani, R. S. Knox, and J. R. Schrieffer, Phys. Rev. Letters **9**, 215 (1962).
[28] F. Herman, J. Callaway, and F. S. Acton, Phys. Rev. **95**, 371 (1954).

Mattheiss[21] showed that the free-electron approximation can underestimate exchange at the low-density atomic tails, and any further reduction of the exchange potential in this region is not justified. In view of these investigations we have used the "bare" Slater free-electron exchange in our calculation. The only justification for this is the good agreement of the Fermi surface found from our energy bands with the experimentally determined Fermi surface of Watts[1] as we discuss in the next section.

3. RESULTS

Energy eigenvalues were computed at 45 points in 1/24 of the Brillouin zone (B.Z.) along major symmetry directions and at points of lower symmetry in the planes ΓKM, ΔUP, and ALH[29] as shown in Fig. 1. The coordinates $\mathbf{k}$ of the grid of points in 1/24 of the B.Z. are given in terms of their components along $\mathbf{b}_1$, $\mathbf{b}_2$, and $\mathbf{b}_3$ of Fig. 1 such that $\mathbf{k}=2\pi[(\alpha/24)\mathbf{b}_1+(\beta/24)\mathbf{b}_2+(\gamma/24)\mathbf{b}_3]$.[30] The eigenvalues are listed in Table II. The coordinates $\mathbf{k}$ at the points of the B.Z. at which the eigenvalues were found are given in the first column in terms of $\alpha/24$, $\beta/24$, $\gamma/24$, and the symmetry labels for some of the irreducible representations are given in the second column. Energy eigenvalues E-versus-$\mathbf{k}$ curves along the major symmetry directions are shown in Fig. 2. These bands represent the $(2s)^2$ electrons of the beryllium atom. The $(1s)^2$ electrons lie approximately 8.9 Ry lower in energy. The ordering of the bands is the same as that of the OPW calculations of Herring and Hill[7] and Loucks and Cutler[11] and are quite similar. As a check on our calculations the lattice constants c and a were increased together and energy eigenvalues were found along the ΓKM directions. We did not bother about convergence or take the trouble to calculate a new potential as the lattice constants were increased. We found that c and a had to be increased by about 200% before beryllium became an insulator. A gap appeared between Γ_4^- and Γ_3^+ with Γ_4^- (s-like) below Γ_3^+ (p-like). K_5 (s-like) fell below K_1 (p-like) and the s-like levels M_1^+ and M_2^- fell below the p-like level M_4^-. These results are only schematic but give us confidence in our calculation. The energy bands have been extended to energy values considerably higher than the Fermi energy E_f than have any previous band calculations to our knowledge. The Fermi energy E_f was determined by the following construction: One plane was drawn midway between the planes ΓKM and ΔUP and another plane was drawn midway between ΔUP and ALH in 1/24 of the B.Z. (Fig. 1). Tiny hexagons were chosen so as to fill up the entire B.Z. and graphically interpolated energies were found at the centers of the small hexagons for the equivalent of 1152 points in the B.Z. with an estimated error of less than 0.01 Ry. Placing the energies in ascending order and counting up to the 2304th energy value gave a Fermi energy $(E_f)=0.84\pm0.01$ Ry measured from the bottom of the band.[31] This interpolated mesh of points in 1/24 of the B.Z. was also used by the author to construct the Fermi surface.[2] The Fermi surface is composed of a hole region in the shape of a coronet and an electron region in the form of two cigars. The hole region arises from the following features of the energy bands [see Fig. 2(a)]: (1) The T_2 state goes above E_f and the T_4 state goes below E_f [see Fig. 2(a)] as one moves from Γ to K. (2) The Σ_3 state goes above E_f while the Σ_1 state goes below E_f as one moves from Γ to M. The electron region arises from the following features of Figs. 2(a) and 2(b): (1) The T_1' state goes below E_f as one moves from M to K while the T_1 state goes below E_f as one moves from Γ to K. (2) The P_1 state goes above E_f as one moves from K to H. P_1 comes into the doubly degenerate (without spin) state H_1 and this determines the height of the cigars.

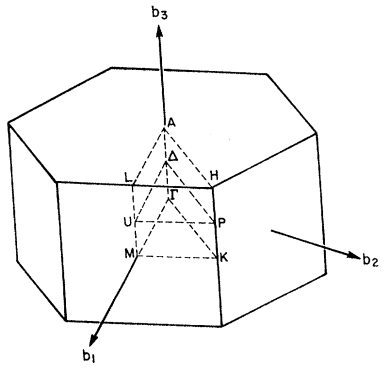

FIG. 1. Brillouin zone for the hcp structure showing 1/24th of the volume in which energy eigenvalues were found.

The hole regions of the theoretically and experimentally determined Fermi surface are in very close agreement, and the major difference lies in the fact that the necks connecting the six corners of the theoretically determined coronet are smaller than the experimentally determined necks as found by Watts. The major area of disagreement between the Fermi surface constructed from the APW band calculation and the experimentally determined Fermi surface of Watts lies in the "cigar-like" electron orbits: the experimental cigars have a slight indentation in the mid-section which is circular; the theoretical cigars also have a slight indentation at the mid-section but have more of a triangular appearance. In addition, the length of the experimental "cigar-like" orbit is longer than the theoretical ones. The major area of disagreement between the Fermi surface found by Loucks and Cutler[11] and the experi-

[29] The notations are those of C. Herring, J. Franklin Inst. 233, 525 (1942).

[30] The reciprocal lattice vectors $\mathbf{b}_1$, $\mathbf{b}_2$, and $\mathbf{b}_3$ satisfy the following relation: $\mathbf{t}_i\cdot\mathbf{b}_j=\delta_{ij}$, $i=1, 2, 3$. In terms of a rectangular coordinate system $\mathbf{b}_1=(2/a\sqrt{3})\hat{\imath}$, $\mathbf{b}_2=(1/a\sqrt{3})(\hat{\imath}+\sqrt{3}\hat{\jmath})$, $\mathbf{b}_3=(1/c)\hat{k}$, where $\hat{\imath}$, $\hat{\jmath}$, $\hat{k}$ are orthonormal unit vectors. $|\mathbf{t}_1|=|\mathbf{t}_2|=a$ and $|\mathbf{t}_3|=c$ are the constants for the hexagonal lattice.

[31] For hcp beryllium there are two atoms/cell and two electrons/atom giving four electrons for each atom in the B. Z. Since a given energy band can accommodate two electrons from each atom in the solid, $(4/2)\times(1152)=2304$ energies will lie below the Fermi energy.

TABLE II. Energy eigenvalues computed by the APW method. The energies are in rydbergs and are measured with respect to the constant value of potential between APW spheres (−1.6998 Ry). The points in k space at which the energy eigenvalues were calculated are given in the first column. See Sec. 3.

$(\alpha/24,\beta/24,\gamma/24)$	Label (if any)	Energy
(0,0,0)	Γ_1^+	−0.0598
	Γ_4^-	0.8401
	Γ_3^+	0.4587
(3/24,0,0)	Σ^1	−0.0267
		0.8518
	Σ^3	1.6657
(6/24,0,0)	Σ^1	0.5017
		0.0725
		0.8656
		1.3271
	Σ^3	0.6272
(9/24,0,0)	Σ^1	0.2358
		0.7438
		1.1876
	Σ^3	1.6475
		0.8315
		1.5147
(12/24,0,0)	M_1^+	0.4046
		1.4941
	M_2^-	0.5450
		1.2321
	M_3^+	1.2398
	M_4^-	1.0364
	M_3^-	1.4214
(2/24,2/24,0)	T_1	−0.0156
		1.6462
	T_2	0.5160
	T_4	0.8554
		1.6672
(5/24,2/24,0)		0.0837
		0.8715
		1.3153
		1.4977
		0.6415
(8/24,2/24,0)		0.2475
		0.7567
		1.1644
		1.3669
		1.6975
		0.8452
		1.5229
(11/24,2/24,0)	T_1'	0.4185
		1.2614
		1.5944
	T_2'	1.2507
	T_3'	1.0510
	T_4'	0.5562
		1.2345
(4/24,4/24,0)	T_2	0.6830
	T_1	0.1170
		1.2528
	T_4	0.8809
		1.4014
(7/24,4/24,0)		0.2818
		0.7939
		1.0535
		1.2827
		1.738
		0.8862
		1.5394
(10/24,4/24,0)	T_1'	0.4582
		1.0536
		1.6574
	T_2'	1.2784
	T_3'	1.0925
	T_4'	0.5872
		1.2388
(6/24,6/24,0)	T_1	0.3377
		0.8999
	T_2	0.9523
	T_3	1.5159
	T_4	0.8364
		1.2588
(9/24,6/24,0)	T_1'	1.7446
		0.5221
		9.8544
		1.6911
	T_2'	1.3026
		1.7406
	T_3'	1.1603
	T_4'	0.6370
		1.2437
		1.7684
(8/24,8/24,0)	K_2	1.6548
	K_3	1.2435
	K_6	1.2534
	K_1	0.5817
	K_5	0.7007
		1.7191
(0,0,6/24)	Δ_1	−0.0193
	Δ_2	0.2949
		1.0947
(3/24,0,6/24)		1.7805
		0.0138
		0.3309
		1.1088
		1.7003
(6/24,0,6/24)		0.1131
		0.4341
		1.1202
		1.3738
		1.6807
		1.6171
(9/24,0,6/24)		0.2748
		0.5728
		0.9320
		1.2132
		1.4735
		1.5070
(12/24,0,6/24)	U_1	0.4388
		0.9462
		1.6729
	U_2	0.5479
		0.9695
	U_3	1.5788
(2/24,2/24,6/24)		1.4691
		0.0252
		1.6929
		0.3436
(5/24,2/24,6/24)		1.7165
		0.1243
		0.4455
		1.1305
		1.3609
		1.5229
(8/24,2/24,6/24)		1.7048
		0.2866
		0.5850
		0.9400
		1.2189
		1.3550
		1.5392

TABLE II (*continued*)

(α/24,β/24,γ/24)	Label (if any)	Energy
(11/24,2/24,6/24)		1.7723
		0.5594
		0.9757
		1.5564
		1.7766
		0.4526
		0.9472
		1.3645
(4/24,4/24,6/24)		1.7160
		0.1575
		1.2899
		1.6906
		0.4789
		1.1492
		1.4191
(7/24,4/24,6/24)		1.7657
		0.3209
		0.6199
		0.9575
		1.1898
		1.2390
		1.5041
(10/24,4/24,6/24)		1.6988
		0.5927
		0.9931
		1.4658
		1.7616
		0.4936
		0.9286
		1.2200
(6/24,6/24,6/24)		1.7538
		0.6676
		1.0691
		1.2374
		1.6910
		0.3764
		0.9326
		1.4205
(9/24,6/24,6/24)		0.6441
		1.0172
		1.3320
		0.5612
		0.8315
		1.1758
(8/24,8/24,6/24)	P_1	1.7796
	P_2	0.6340
	P_3	1.0317
		0.7009
		1.2225

(α/24,β/24,γ/24)	Label (if any)	Energy
(0,0,12/24)	A_1	0.1014
		1.5347
(3/24,0,12/24)	R_1-R_3	0.1322
		1.5536
(6/24,0,12/24)	R_1-R_3	0.2319
		1.3905
(9/24,0,12/24)	R_1-R_3	1.6970
		0.3900
		1.0571
(12/24,0,12/24)	L_1	0.5131
	L_2	0.8680
(2/24,2/24,12/24)	S	1.6037
		0.1463
(5/24,2/24,12/24)		1.5403
		0.2523
		1.5829
(8/24,2/24,12/24)		1.7675
		0.4128
		1.0727
(11/24,2/24,12/24)	S'	1.5520
		0.5280
		0.8696
(4/24,4/24,12/24)	S	1.5172
		0.2791
		1.3835
		1.4748
(7/24,4/24,12/24)		1.7793
		0.4333
		1.0715
(10/24,4/24,12/24)	S'	1.3905
		0.5696
		0.8676
(6/24,6/24,12/24)	S	1.3611
		0.4897
		1.0237
		1.2900
(9/24,6/24,12/24)	S'	0.6366
		0.8401
		1.2376
(8/24,8/24,12/24)	H_1	0.7865
	H_2	1.1965
	H_3	0.6990

mentally determined Fermi surface according to Watts also arises from the "cigar-like" electron orbits. Instead of an indentation at the mid-section of the cigars, Loucks and Cutler found a definite bulge. Loucks[32] later showed, however, that the "waists" in the "cigars" were in fact a feature of the OPW band calculation of Loucks and Cutler.[11] The length of the theoretical "cigars" still continued to remain shorter than the experimental ones. Thus, the band calculations presented here and of Loucks and Cutler both give rise to nearly identical Fermi surfaces, both differing in nearly the same way from the experimentally determined Fermi surface of Watts.

[32] T. L. Loucks, Phys. Rev. 134, A1618 (1964).

A density-of-states curve is shown in Fig. 3. This is a histogram which was constructed by dividing the ordered energies into increments ΔE and counting the number of states in each ΔE. The value $\Delta E=0.08$ Ry was a compromise between detail and smoothness. The smooth curve in Fig. 3 is drawn so that the area under each square is approximately constant. The density of states according to Herring and Hill is the dashed curve in Fig. 3. Our density of states, which is similar to the one of Loucks and Cutler, has more structure than does that of Herring and Hill, but does not have as much structure as the one given by Cornwell,[13] who used a psuedopotential method for obtaining the energy levels at a few symmetry points. It is customary to compare

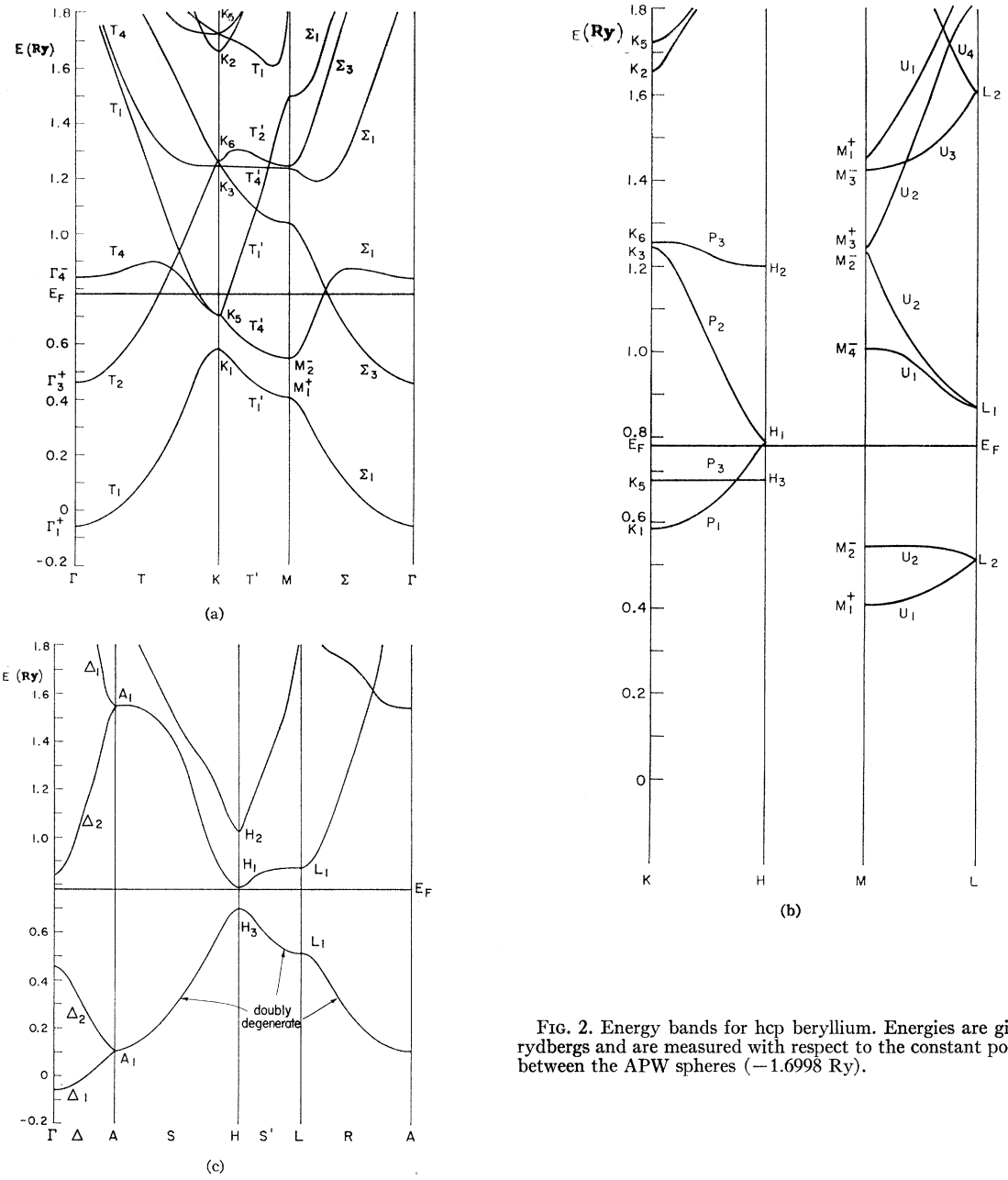

FIG. 2. Energy bands for hcp beryllium. Energies are given in rydbergs and are measured with respect to the constant potential between the APW spheres (−1.6998 Ry).

the calculated bandwidth with the soft-x-ray emission data, although not much importance can be attributed to this because of the low-energy tail of the x-ray data. Johnston and Tomboulian[3] have found that the x-ray absorption edge coincides with the high-energy limit of the emission line in beryllium and that the absorption data have a peak at the low-energy end. These results are consistent with Fig. 3. Since the bands for $E>E_f$ have been found, it would be interesting to extend the density of states to higher energies so that comparison with the x-ray absorption data of Johnston and Tomboulian could be made. The density of states at the Fermi energy, $N(E_f)$, gives us the electronic specific heat. We cannot say anything very conclusive about the value of the electronic specific heat we find from our density of states, since E_f intersects a very steep portion of the density-of-states curve, and $N(E_f)$ is sensitive to the construction of the histogram. Very roughly, we find that γ lies between 0.3×10^{-4} and 0.5×10^{-4} (cal/°K² mole). Hill and Smith[4] found $\gamma=0.54\times10^{-4}$ (cal/°K² mole) while more recently, Gmelin[5] found $\gamma=(0.44\pm0.04)\times10^{-4}$ (cal/°K² mole).

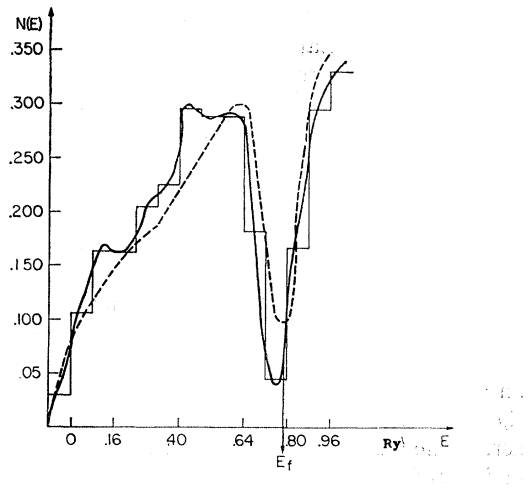

FIG. 3. Density of states for beryllium. Solid curve found using results of APW band calculation. The dashed curve is taken from Herring and Hill (Ref. 7). $N(E)$ = No. elecs/(atom)(0.08 Ry).

4. DISCUSSION

In this section we will compare qualitatively the band structure of hcp beryllium to the band structure of hcp magnesium from the viewpoint of the APW method. This is achieved by comparing the logarithmic derivatives of beryllium and magnesium for one APW wave function at their respective APW sphere radii. This comparison enables us to understand the differences between the Fermi surfaces of beryllium and magnesium. We next discuss the APW method in the light of the OPW cancellation theorem of Cohen and Heine.[15]

It is requried that the trial solutions in the APW method be plane waves in the constant-potential region between the spheres which match in value the general spherical solutions to the Schrödinger equation inside the spheres of radius R_s. Slater[20] has discussed the APW method from the viewpoint of scattering theory and has shown that the diagonal APW matrix element can be written approximately in a form which exhibits the energy dependence as the difference between the logarithmic derivatives $u_l'(R_s,E)/u_l(R_s,E)$ and $j_l'(kR_s)/j_l(kR_s)$ at R_s. $u_l(R_s,E)$ is the solution of the radial Schrödinger equation for angular momentum l and energy E using the crystalline potential, while $j_l(kR_s)$ is the spherical Bessel function of angular momentum l which comes from the familiar series expansion for the plane wave. It turns out that if for some k the logarithmic derivatives are approximately equal, then the electron bands are approximately free.

The logarithmic derivatives for beryllium and magnesium are shown in Figs. 4 and 5.[33] The potential of Falicov[6] (modified slightly for the APW method) was used for magnesium and the potential of Table II was used for beryllium. The zero of energy ($k=0$) was chosen at the bottom of the band and the abscissa was determined from the condition $E=k^2$. The curves show that: (1) As l increases, the difference between the logarithmic derivatives at R_s decreases, and (2) matching is better for magnesium than for beryllium.

When the matching at R_s is poor, we may regard the linear combination of APW functions needed for convergence in energy as providing scattered wavelets. This scattering corresponds physically to the absence of the "anti-resonance" in energy of slow incident electrons scattering off the spherical APW potential. This is analogous to the Ramsauer-Townsend effect as has been emphasized by Slater.[20]

We point out that this discussion is related to the psuedopotential method of Heine and Abarenkov[16] for calculating electronic structures of nontransition metals. In setting up the potential seen by a conduction electron in a metal, they discuss separately the potential of the electron inside the ion core of one of the atoms and the potential in the region between the ions. The potential in the region between the ions was obtained by a dielectric screening calculation following Cohen and Phillips[34] while the potential inside the ion core was fitted to the spectroscopically measured energy levels of the free ion in the spirit of the quantum-defect method of Ham.[35] However, as Kuhn and Van Vleck[36] showed, the logarithmic derivative of the wave function at the surface of a suitably defined sphere (analogous to the APW sphere of radius R_s), which surrounded the ion was all that was necessary to obtain the band structure.

The differences in the logarithmic derivatives between beryllium and magnesium shown in Figs. 4 and 5, no doubt go a long way toward explaining the fact that the bands, and consequently the Fermi surface of

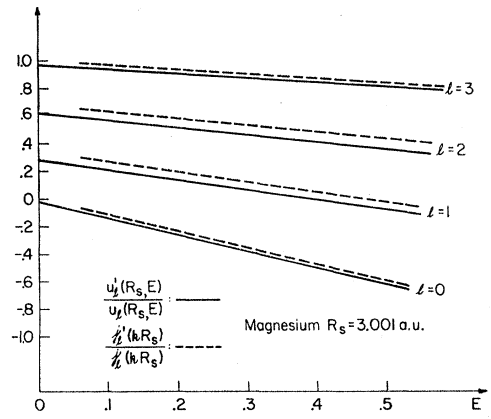

FIG. 4. Logarithmic derivatives of the radial wave functions $u_l(R_s,E)$ and the spherical Bessel functions $j_l(kR_s)$ as a function of energy (E) for magnesium. The abscissa is determined from the relation $E=k^2$ and is in rydbergs.

[33] The author wishes to thank J. F. Kenney for the use of his computer program to generate the $j_l'(kR_s)/j_l(kR_s)$.

[34] M. H. Cohen and J. C. Phillips, Phys. Rev. **124**, 1818 (1961).
[35] F. S. Ham, Solid State Phys. **1**, 127 (1955); Phys. Rev. **128**, 82 (1962); **128**, 2524 (1962).
[36] T. S. Kuhn and J. H. Van Vleck, Phys. Rev. **79**, 382 (1950).

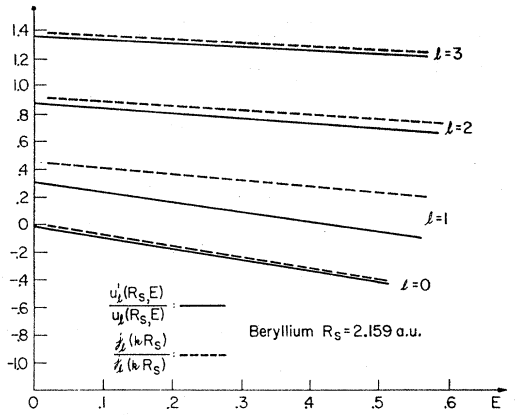

FIG. 5. Logarithmic derivatives of the radial wave functions $u_l(R_s,E)$ and the spherical Bessel functions $j_l(kR_s)$ as a function of energy (E) for beryllium. The abscissa is determined from the relation $E=k^2$ and is in rydbergs.

magnesium, are more free-electron-like than is the case for beryllium. The Fermi surface of magnesium has been found by Falicov[6] by the OPW method and more recently by Dimmock, Freeman, and Furdyna[37] by the APW method. Both calculations showed that the Fermi surface was very close to the free-electron Fermi surface constructed by Harrison.[10] We have already noted that distortions in the free-electron Fermi surface occur for the case of beryllium.

Consider next these results from the viewpoint of the OPW cancellation theorem of Cohen and Heine.[15] The OPW cancellation theorem says roughly that the effective potential $V(r)$ acting on an electron in a metal is cancelled in strength in proportion to how well the bound states form a complete set in the region where $V(r)$ is large. From this it follows that there is no cancellation of a level l' when none of the core levels are l'-like. Since there is no p-core level of the beryllium atom, one expects the cancellation to be poor. Magnesium, on the other hand, has a neon core and the theorem says we may expect more cancellation.

The matching of logarithmic derivatives across R_s in the APW scheme and the OPW cancellation theorem are describing the same physical situation: (consider beryllium).

(1) The absence of a p shell in the OPW scheme means there will be no cancellation of $V(r)$ for p levels. In the APW scheme one expects the difference in logarithmic derivatives at R_s for $l=1$ to be large.

(2) Since for large l the centrifugal potential term in the Schrödinger equation excludes bound states from the interior region of $V(r)$, the effective potential $V(r)$ acting on an electron in a metal is not being effectively cancelled in the OPW scheme. In the APW scheme the centrifugal potential term causes bound states to be excluded from the region of the APW sphere of radius R_s and the $u_l(R_s,E)$ becomes more plane-wave-like. This provides better matching with the plane waves outside the sphere of radius R_s.

The OPW method is provided with a useful device for reasoning in the form of the cancellation theorem of Cohen and Heine. An analogous theorem from the viewpoint of the APW method does not exist. Since the Cohen and Heine OPW cancellation theorem is derived from a variational statement which requires that the effective potential acting on an electron be a minimum, an analogous theorem in the APW scheme might take the form of a variational statement on the phase shift across the APW sphere radius R_s. This is at present under study.

5. SUMMARY

The results of an APW band calculation for hcp beryllium have been presented in the form of the Fermi energy, the energy bands which were extended to energies much greater than the Fermi energy, the density-of-states curve below the Fermi energy, and the electronic specific heat. The energy bands were found to be quite similar to the bands found by Herring and Hill and Loucks and Cutler. The potential used in obtaining the energy bands was constructed by superposing atomic-beryllium potentials on first-, second-, and third-nearest neighbors while exchange was treated in the Slater free-electron-exchange appropriation. The density-of-states curve compared favorably to the x-ray emission data of Johnston and Tomboulian, and the electronic specific heat was found to be in reasonable agreement with the published experimental results.

The Fermi surface was described in terms of the intersections of the Fermi energy with the energy bands and a qualitative comparison with the experimentally determined Fermi surface found by Watts was made. The logarithmic derivatives for one APW wave function at the APW sphere radius R_s were found for beryllium and magnesium, and these results were compared from the viewpoint of the OPW cancellation theorem of Cohen and Heine. We also indicated that the APW method is related to the pseudopotential method of Heine and Abarenkov.

ACKNOWLEDGMENTS

It is a pleasure to express my gratitude to Dr. L. F. Mattheiss of the Bell Telephone Laboratories for his vital collaboration in the early phase of this work and for a critical reading of the manuscript, and to Professor J. H. Wood of MIT for helpful discussions and suggestions.

[37] J. O. Dimmock, A. J. Freeman, and A. M. Furdyna, Bull. Am. Phys. Soc. **10**, 377 (1965).